Latent addition in motor and sensory fibres of human peripheral nerve

H. Bostock and J. C. Rothwell

The Institute of Neurology, Queen Square, London WC1N 3BG, UK

1. The time constants of motor and sensory nerve fibres were studied in normal human ulnar nerves by the method of latent addition, using threshold tracking to follow the recovery of excitability after brief conditioning current pulses. The 60 μs test and conditioning stimuli were applied at the wrist, and the conditioning stimuli were set to 90, 60, 30, −30, −60 and −90% of the control threshold current. Compound muscle action potentials were recorded from abductor digiti minimi, and sensory nerve action potentials from the little finger.

2. Recovery from depolarizing conditioning pulses was slower than recovery from hyperpolarizing pulses and strongly dependent on conditioning pulse amplitude. The voltage dependence of latent addition was attributed to subthreshold activation of sodium channels (local response).

3. Motor and sensory nerve excitability generally recovered from −90% hyperpolarizing pulses as the sum of two exponential components, although the slow component was negligible in some motor nerves. The fast component (time constant 43·3 ± 2·0 μs, mean ± S.E.M., $n = 9$) was similar between motor and sensory fibres in the same subject. It showed no consistent voltage dependence, and was attributed to a passive input time constant of the fibres. The slow component of recovery from hyperpolarizing pulses was greater in sensory than in motor fibres and was voltage dependent: it could be greatly increased in motor and sensory fibres by steady depolarization. It was attributed to a regenerative membrane current, active at the resting potential in sensory and at least some motor nerves.

4. The latent addition responses were compared with the computed responses of four theoretical models. Both motor and sensory responses were well fitted by a model in which a fraction of the sodium channels (less in motor than in sensory fibres) were activated at potentials 20 mV more negative than normal and at half the normal rate, and did not inactivate.

5. It is concluded that the differences in latent addition between motor and sensory fibres are primarily due to differences in non-classical, voltage-dependent ion channels, active close to the resting potential. These 'threshold channels' may help to account for the longer strength–duration time constant of sensory fibres, for their lower rheobase, and for their greater tendency to fire repetitively.

It is now well established that the sensory fibres in human peripheral nerve have a longer strength–duration time constant than the motor fibres (Panizza, Nilsson, Roth, Basser & Hallett, 1992; Mogyoros, Kiernan & Burke, 1996), where the strength–duration time constant is an apparent membrane time constant, derived from the relationship between the strength and duration of the stimulus required to excite action potentials. Rheobase is the minimal current strength which, when applied for a long duration, is sufficient to excite an action potential. Since sensory fibres also tend to have a lower rheobase than motor fibres (Mogyoros *et al.* 1996), it is therefore often possible to activate sensory nerve action potentials and H reflexes preferentially with long duration (e.g. 1 ms) current pulses, and motor nerve action potentials with brief (e.g. 50 μs) stimuli (e.g. Veale, Mark & Rees, 1973; Panizza, Nilsson & Hallett, 1989; Panizza *et al.* 1992). The reason for this difference is not known, but Panizza, Nilsson, Roth, Rothwell & Hallett (1994) compared motor and sensory nerve time constants by the method of latent addition (cf. Tasaki, 1950). They applied 50 μs conditioning pulses, set to 50 or 90% of threshold for a standard, submaximal response, and measured the time constant of the decay in the change in threshold to a second 50 μs pulse. They found that the time constants were similar to the strength–duration time constants measured for the same nerves, and showed a similar difference between motor and sensory fibres: sensory fibres had time constants that were about 3 times longer than those of motor fibres (Panizza *et al.* 1994). They concluded that there must be a difference in passive

membrane time constant between motor and sensory fibres. However, the use of near-threshold depolarizing conditioning pulses raised the possibility of a contribution of local responses to the excitability changes (Katz, 1937), due to subthreshold activation of sodium channels. The time constants measured with the 90% conditioning pulses were invariably longer than those measured with 50% pulses. To clarify this matter, we have reinvestigated the latent addition phenomena in human peripheral nerve, extending our observations to hyperpolarizing as well as depolarizing conditioning pulses of different sizes. We have also used mathematical modelling to help interpret our results. We have found evidence that the motor–sensory differences in recovery times depend on active rather than passive membrane properties, and modelling suggests that a non-classical sodium conductance is particularly important. A preliminary account of this study has been presented (Bostock & Rothwell, 1995).

METHODS

Human nerve recording

Latent addition was studied in ten healthy volunteers, aged 25–51 years, with informed consent and the approval of the local ethical committee. All the subjects were clinically normal, but one was known to have unusually excitable motor nerves, as indicated by a positive Trousseau's sign (fasciculations during ischaemia), and his results were handled separately.

The ulnar nerve was stimulated at the wrist through a non-polarizable surface electrode (Red Dot, 3M Canada Inc., London, Ontario, Canada) with a remote indifferent electrode. Stimuli were generated by a purpose-built isolated current source with a maximal output of 50 mA, driven by an IBM 486DX computer, running QTRAC software (copyright Institute of Neurology). Compound motor action potentials (CMAPs) were recorded from the skin over abductor digiti minimi, or compound sensory nerve action potentials (SNAPs) from the little finger, with surface electrodes. The procedure for recording latent addition was similar to that used for recording 'threshold electrotonus' (Bostock, Sharief, Reid & Murray, 1995), differing only in the timing of the pulses and the amplitudes of the conditioning pulses. A target response was set to 30–40% of the maximal response to a 60 μs current pulse, and the 'control threshold' determined as the current required to elicit the target response. The nerve was tested at 2 Hz, and eight stimulus conditions tested in turn: test stimulus alone (control) and test stimulus added to a 60 μs 'conditioning' pulse set to 90, 60, 30, 0, −30, −60 and −90% of the last control stimulus. The starting time of the conditioning pulses was stepped from 0·2 ms after the test pulse to 0·5 ms before it in steps of 20 μs, over a period of about 10 min (e.g. Fig. 1). (We extended this study to conditions in which the conditioning stimulus followed the test stimulus by up to 200 μs, because this aspect of latent addition was one which most clearly revealed the inadequacies of the simplest models.) In most experiments the tracking procedure was different from that used previously, in that the change in stimulus current was made *proportional* to the difference between the recorded response and the target response. Thus if a response was only 50% of the target response, the next stimulus for the same stimulus condition would typically be increased by 5%; if the response was 10% greater than target, the stimulus would be decreased by 1%, etc. For each interstimulus interval, the conditioned threshold was estimated by averaging the stimulus currents (weighted towards the last values), and percentage threshold changes were calculated as: (conditioned threshold − control threshold)/(control threshold) × 100. For each conditioning current, the recovery time of latent addition was defined as the time taken for the threshold change to decay to 1/e of its maximum value, and estimated by linear interpolation between successive intervals.

Exponential fitting. To fit a single exponential (of the form $y = Ae^{-x/\tau}$, where A and τ are constants) to the recovery from hyperpolarizing responses, a straight line was first fitted to the logarithms of the threshold changes for delays between 0·04 and 0·5 ms, for threshold changes between 1 and 100% of maximum, weighting each data point in proportion to the threshold change. The parameters A and τ were then optimized by making repeated small changes to minimize the sum of the squares of the differences between the original threshold changes and the fitted exponential. To fit two exponentials (of the form $y = A_1e^{-x/\tau_1} + A_2e^{-x/\tau_2}$), a single exponential was first fitted to the delays from 0·2 to 0·5 ms (as above); this estimated slow component was subtracted from the threshold changes, and a second exponential fitted to the differences. The four parameters A_1, A_2, τ_1 and τ_2 were then optimized iteratively as before.

Models of latent addition in myelinated axons

The latent addition recordings were compared with computer simulations for four theoretical model axons. For the excitable models (models 2–4), the resting potential was first determined as the potential for zero membrane current, and then the control threshold current was estimated by trial and error as the current required just to generate a spike (defined as a membrane potential > -20 mV) within 500 μs of the end of a 60 μs test stimulus. Conditioning pulses were then set to amplitudes from 90 to −90% of the control threshold current, and the conditioned threshold current determined to within 0·5% for conditioning pulses applied at 5 μs intervals from 0·2 ms after to 0·5 ms before the test stimulus, to generate latent addition curves comparable to those determined experimentally from the human nerves (Fig. 7). The membrane potential and sodium current due to the conditioning pulses alone were also plotted. The models were implemented in Microsoft Basic on a 486DX, IBM-compatible PC.

Model 1. This was equivalent to a simple resistance–capacitance (RC) circuit, as assumed by Panizza *et al.* (1994), but with the time constant set close to the fast time constant for the latent addition to hyperpolarizing currents in the human nerves ($\tau = 45$ μs). This model contained no voltage-dependent elements, so to produce a figure comparable to those for models 2–4, the resting potential was set to −86·7 mV, the same as for model 2, and a spike was arbitrarily defined as a depolarization to −60 mV. The latent addition responses for model 1 are made up of a series of curves, for which explicit expressions can be derived (see Appendix).

Model 2. This model incorporated nodal voltage-dependent sodium and slow potassium channels, and was derived from the human motor axon model used previously (Bostock, Burke & Hales, 1994). The apparent nodal resistance for the brief pulses used in this study was determined in part by the nodal potassium channels, but mainly by the 'internodal leak resistance' (R_{il}), representing current paths to the internodal axolemma through and underneath the myelin (Barrett & Barrett, 1982; Bostock, Baker & Reid, 1991). For the simulations of latent addition over 0·5 ms, however, the membrane potential of the internodal axolemma and the activation of the nodal slow potassium channels were effectively constant, so that this model was equivalent to a simple RC membrane with the addition of sodium channels. The sodium channel kinetics were

taken from the model of Schwarz & Eikhof (1987), based on voltage clamp recordings from rat nodes of Ranvier. The input capacitance (C_{in}, comprising nodal and myelin components) and R_{ll} were adjusted to give a passive time constant similar to model 1 (i.e. $C_{in} = 1{\cdot}9$ pF, $R_{ll} = 25$ MΩ). Internodal sodium channels were omitted.

Model 3. This was the same as model 2, but with sodium channel kinetics and voltage dependence taken from Schwarz, Reid & Bostock (1995), based on observations on nodes of Ranvier from human peripheral nerve. Since the altered sodium channels slightly affected the responses to hyperpolarizing as well as depolarizing pulses, R_{ll} was reduced further to 20 MΩ to maintain the fast time constant close to 45 μs.

Model 4. This was the same as model 3, but with a variable proportion of sodium channels replaced by 'threshold channels', which had activation (m) parameters shifted 20 mV more negative and slowed by a factor of 2, and which did not inactivate. These properties of the 'threshold channels' are similar to those of the Na_P (persistent sodium) channels in a model of cerebellar Purkinje cells (de Schutter & Bower, 1994).

Estimations of strength–duration time constant and rheobase

The strength–duration relationship for myelinated axons normally obeys Weiss's law, i.e. stimulus charge increases linearly with stimulus duration (Tasaki, 1939; Bostock, 1983; Bostock, Sears & Sherratt, 1983) and this relationship has recently been confirmed for human motor and sensory fibres *in vivo* (Mogyoros *et al.* 1996). We used Weiss's law to estimate the strength–duration time constant and rheobase from thresholds at two different stimulus durations, 60 and 600 μs, as done by Bostock & Bergmans (1994). Thus, if I_t is threshold current for a stimulus of duration t, ρ is rheobase and τ is the strength–duration time constant, then:

$$I_t t = \rho(t + \tau), \qquad \text{(Weiss's Law)}$$

i.e.

$$I_{60}60 = \rho(60 + \tau),$$

$$I_{600}600 = \rho(600 + \tau).$$

Hence:

$$\rho = (10I_{600} - I_{60})/9,$$

$$\tau = 600(I_{60} - I_{600})/(10I_{600} - I_{60}).$$

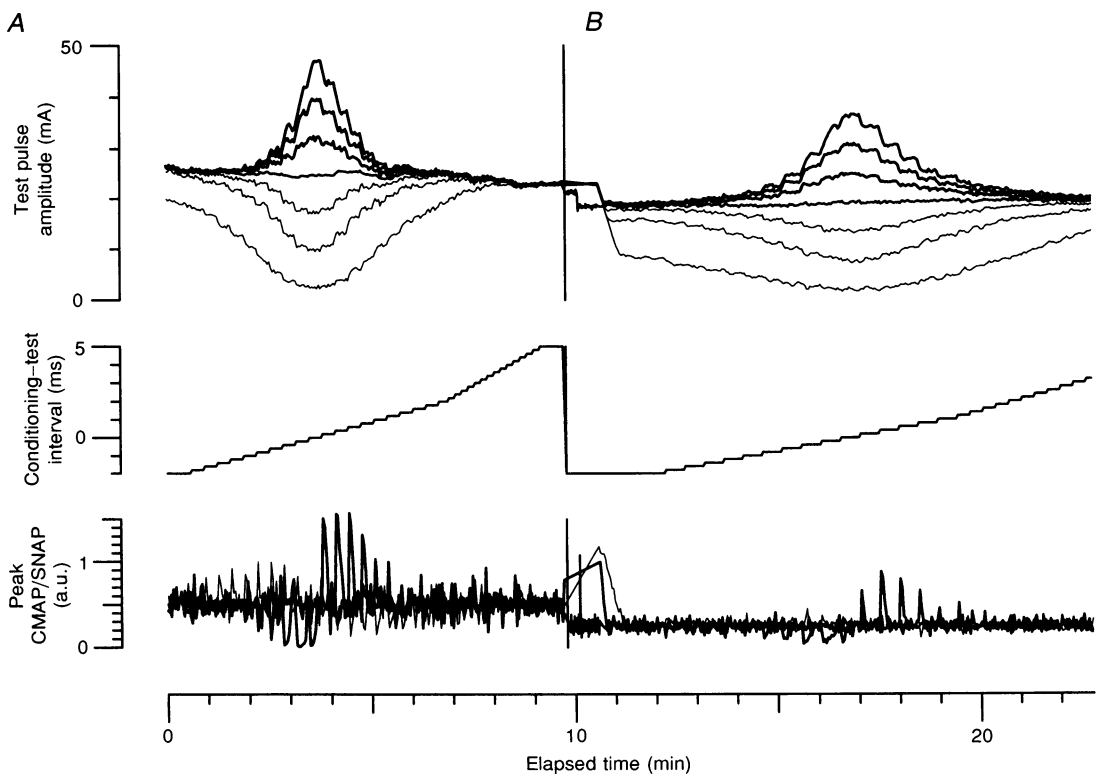

Figure 1. Latent addition recordings in real time

Latent addition recorded from motor fibres (*A*) and sensory fibres (*B*) in the ulnar nerve of a normal subject. Vertical line indicates time when excitability testing was interrupted and responses switched from CMAP to SNAP. Top: test pulse amplitudes (threshold currents) adjusted to produce 40% maximal responses, for test stimuli delivered alone, and for conditioning stimuli set to −90, −60 and −30% (thicker lines), and 30, 60 and 90% (thinner lines) of the last control test stimulus amplitude. Middle: delay between conditioning and test pulses, stepped from −0·2 ms (i.e. conditioning pulse after test pulse) to 0·5 ms in 20 μs steps. Bottom: peak action potential amplitudes (a.u., arbitrary units), showing operation of threshold tracking. Data from control and ±90% channels superimposed, with line thickness as at top. The largest excursions were for the −90% (hyperpolarizing) conditioning pulses.

RESULTS

Latent addition *in vivo*

Full curves for latent addition to 60 μs pulses from 90 to −90% of threshold in steps of 30% are plotted in Fig. 2, for CMAP (*A*) and SNAP (*B*) in a normal subject. It is clear that for each type of fibre the depolarizing pulses (lower curves) have more long-lasting effects than the hyperpolarizing pulses (upper curves), and that the sensory fibres recover more slowly than the motor fibres. The recovery times to 36·8% (1/e) of the maximum threshold change are plotted as a function of the strength of the conditioning pulse in Fig. 2*C*. Similar results were obtained for eight other normal subjects with no known nerve abnormality, and the means and standard errors are plotted in Fig. 2*D*. The recovery times to the 90% depolarizing pulses are comparable with the figures for the time constant given by Panizza *et al.* (1994), but much longer than the recovery times to the hyperpolarizing pulses, suggesting that they depend on sodium channel activation (local response) as well as the membrane time constant. However, it is also clear that the recovery of the sensory fibres to hyperpolarizing, as well as depolarizing pulses, is slower than for the motor fibres, so that the motor–sensory difference cannot be explained simply on the basis of sodium channels activated by depolarization.

Fast and slow components of hyperpolarizing responses

According to our first three models (see below), the responses in the 1st (top right) quadrant, i.e. following hyperpolarizing pulses, should approximate closely to an exponential decay, corresponding to the passive membrane time constant of the fibres. Accordingly, in Fig. 3, which illustrates (*A* and *B*) the latent addition results corresponding to the raw data in Fig. 1, the −90%, 1st quadrant responses are plotted on a logarithmic scale (*C* and *D*). The CMAP results (Fig. 3*C*) fall on a straight line, indicating an exponential decay with a time constant of 45 μs. The sensory points (Fig. 3*D*), however, were fitted much better by curved lines, corresponding to the sum of two exponentials, with time constants of 46 and 218 μs. The faster sensory time constant was remarkably similar to the motor one. In two other subjects the −90% motor response was also well fitted by a single exponential, but for the remaining subjects there was an appreciable slow component in the motor as well as the sensory responses. The most extreme example is illustrated in Fig. 4 for the subject

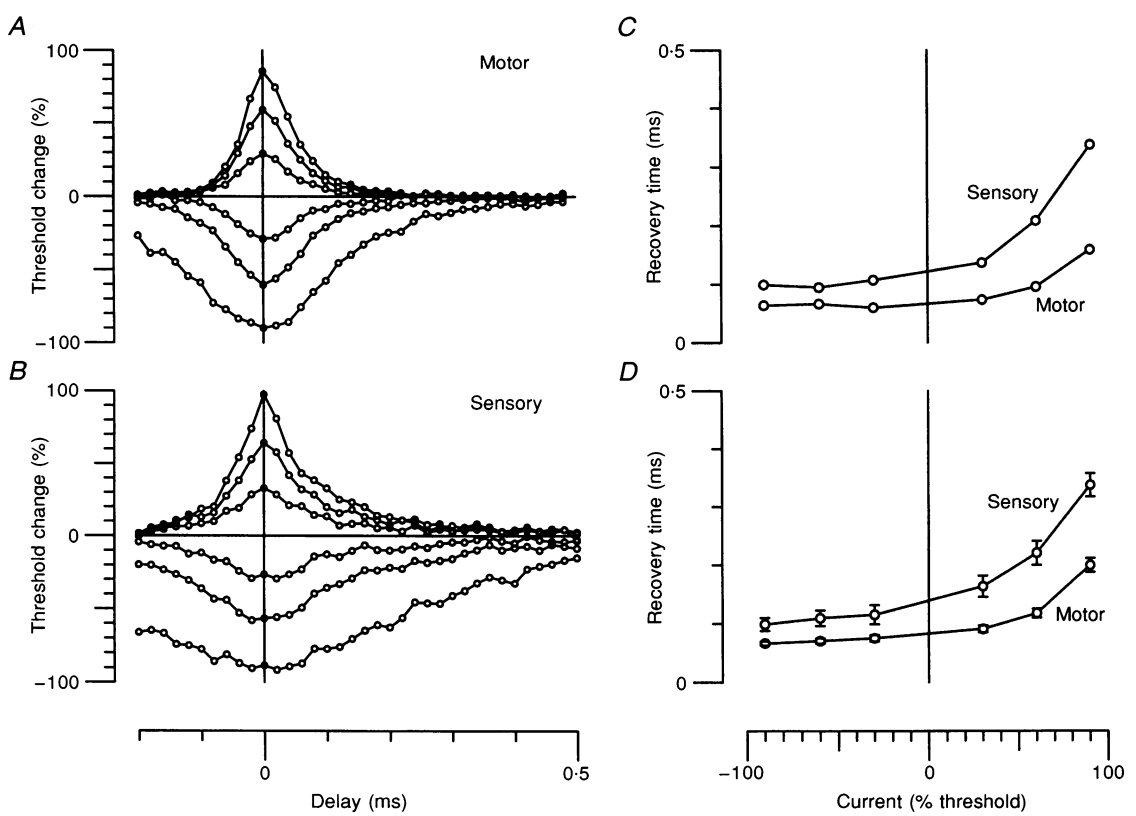

Figure 2. Motor and sensory latent addition

Latent addition in motor (*A*) and sensory (*B*) fibres of normal subject (different subject from Fig. 1). Each point represents estimated conditioned threshold current, expressed as percentage change from unconditioned threshold, plotted against delay between conditioning and test stimuli. *C* and *D*, recovery times, estimated as delays for threshold change 1/e of maximum, plotted for motor and sensory action potentials as indicated. *C*, data from recordings in *A* and *B*. *D*, averaged data for 9 normal subjects (means ± S.E.M.).

exhibiting a mild Trousseau's sign, and for whom latent addition was very similar in motor and sensory axons. The motor and sensory −90% responses have both been fitted with the sum of two exponentials which gave the best least-squares fit, and they were each separated into similar fast and slow components.

Since neither fast nor slow time constant (where measurable) appeared significantly different between motor and sensory fibres in the same subject, and a slow component could not be measured in all motor responses, we estimated fast and slow time constants for each subject by fitting two exponentials to the sum of the motor and sensory responses. The fast motor/sensory time constants obtained in this way averaged 43·3 ± 2·0 μs (mean ± S.E.M., $n = 9$), while the slow time constants averaged 175 ± 21 μs. The fast time constants differed much less between subjects, as well as between motor and sensory fibres, than the recovery times, and were close to estimates of the nodal time constant reported for isolated (Schwarz & Eikhof, 1987; Schwarz *et al.* 1995) or functionally isolated (Brismar, 1981) mammalian fibres. Our supposition that the fast time constants correspond approximately to the passive input time constants of the fibres was supported by modelling (see below).

Although the slow components of latent addition to hyperpolarizing pulses were well fitted by exponentials up to 0·5 ms, we had no reason to suppose that they were caused by a truly exponential decay process. To quantify the slow components we therefore simply estimated the threshold change at 0·2 ms, a time when the fast component had decayed to about 1% of its maximum value. Slow components measured in this way are compared in Table 1 for motor and sensory responses to the three different sized hyperpolarizing pulses. There was considerable variation between subjects, but Student's paired t tests showed that not only were the slow components consistently larger in sensory than motor fibres, but also that for both motor and sensory fibres the slow components, when expressed as a percentage of the maximum threshold change, were significantly smaller for the −90% than for the −30% hyperpolarizing pulses. In other words, the slow components of latent addition, not attributable to the nodal time constant, were voltage dependent.

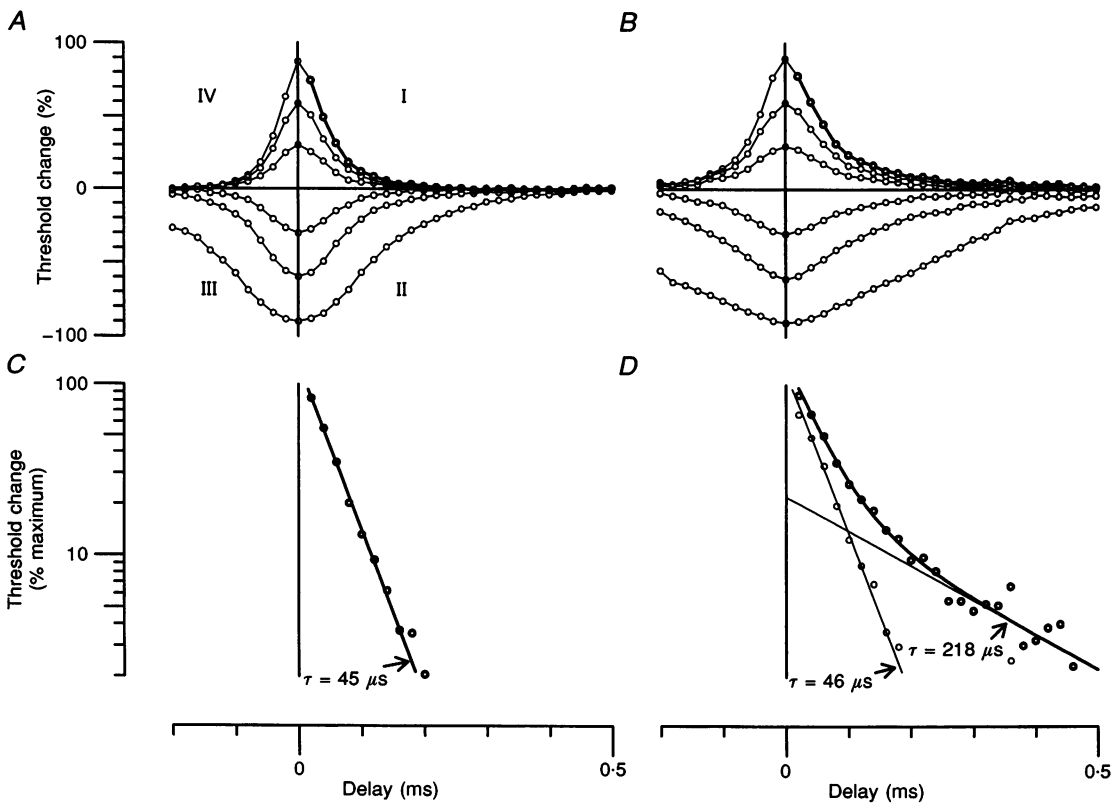

Figure 3. Exponential components of latent addition

Latent addition data for motor (*A*) and sensory (*B*) fibres (same experiment as Fig. 1), plotted as in Fig. 2*A* and *B*. Roman numerals indicate 1st–4th quadrants referred to in text. Thick lines and circles: responses to −90% (hyperpolarizing) conditioning stimuli selected for curve fitting and replotted in *C* and *D*. *C* and *D*, −90% (hyperpolarizing) responses from *A* and *B* (1st quadrant) replotted on logarithmic scale. Line in *C* and curve in *D* are best fit single and double exponentials, respectively (see text). In *D*, the thin lines are the separate fitted fast and slow exponential components, and the thin circles are the data points after subtraction of the slow component.

Table 1. Slow components of latent addition to hyperpolarizing pulses

	−90%	−60%	−30%	(−30%)−(−90%)
Motor	4·92 ± 0·78	6·17 ± 0·89	7·26 ± 1·13	2·36 ± 0·46**
Sensory	15·6 ± 2·9	17·7 ± 2·6	20·0 ± 2·5	4·3 ± 0·58**
Sensory − motor	10·7 ± 2·2*	11·5 ± 2·4*	12·7 ± 2·3**	—

*$P < 0·005$, **$P < 0·001$ (Student's two-tailed paired t test). Threshold changes at 0·2 ms (estimated by fitting two exponentials), expressed as a fraction of maximum threshold change, averaged over 9 subjects. All values are the mean ± S.E.M.

Effects of membrane polarization on latent addition *in vivo*

To demonstrate the voltage dependence of the slow component more directly, in three subjects we superimposed the normal latent addition pulses on 20 ms depolarizing or hyperpolarizing currents. The polarizing currents were set to ±50% of the threshold current for a 1 ms pulse (see Methods). Figure 5 illustrates the effects of polarization on latent addition in motor fibres, in a subject who had only a small slow component at rest. This was abolished by hyperpolarization (Fig. 5*A*), so that the −90% response was well fitted by a single exponential (Fig. 5*C*). Depolarization, on the other hand, prolonged latent addition and induced a prominent slow component, so that the responses closely resembled those from unpolarized sensory fibres (Fig. 5*B* and *D*). Polarization had no appreciable effect on the time constant of the fast component (Fig. 5*C* and *D*). Similar effects of polarization on latent addition were observed in the other two subjects.

To test if the voltage dependence of the slow component of latent addition was related to the voltage dependence of the strength–duration time constant, previously reported by Bostock & Bergmans (1994), we estimated both parameters concurrently, while applying polarizing currents of different amplitudes. The slow component of latent addition was measured 0·2 ms after a −90% conditioning pulse, while the strength–duration time constant was estimated by comparing thresholds to 60 and 600 μs test pulses (see

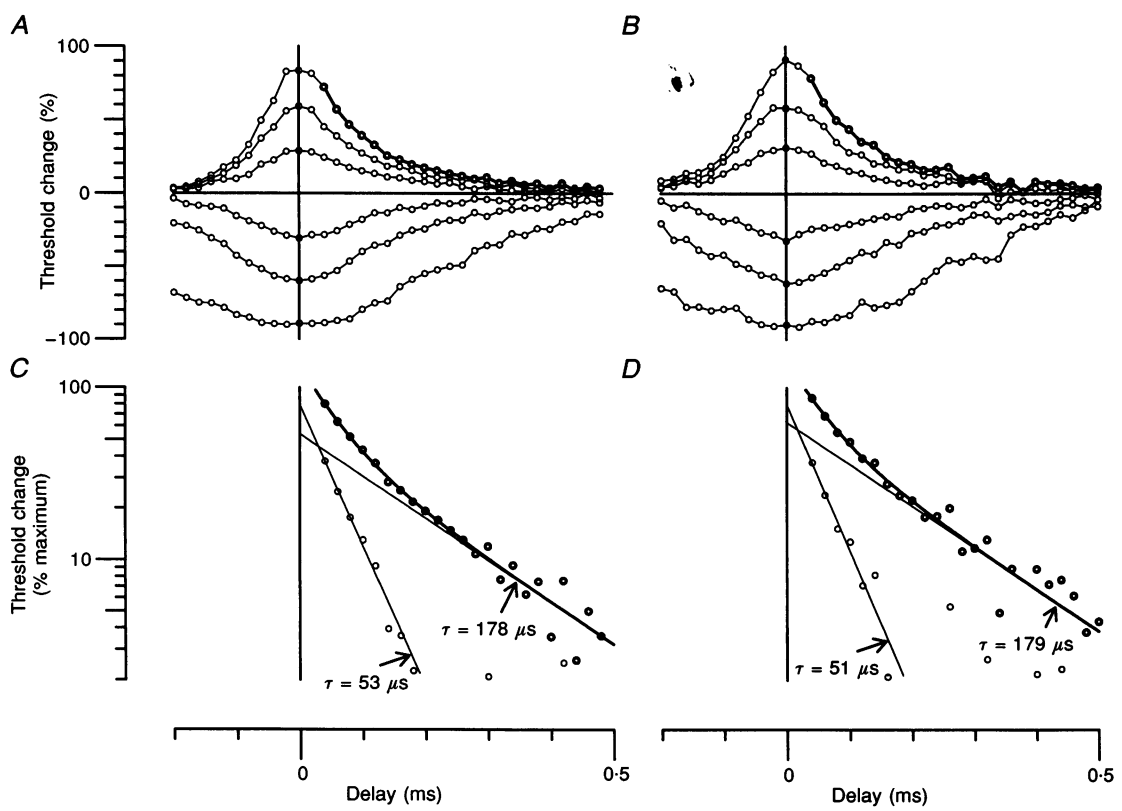

Figure 4. Motor fibres can also have a slow component

Latent addition and exponential components, plotted as in Fig. 3, for subject with mild Trousseau's sign showing unusually little difference between motor and sensory nerve excitability.

Methods). Polarizing currents were applied for 20 ms before and during the test pulses, and defined as before in relationship to the threshold for a 1 ms current pulse. The results are illustrated in Fig. 6 for motor and sensory fibres in the same subject as in Fig. 5. Strength–duration time constants, always longer in the sensory than the motor fibres, were varied over a wide range by polarization (Fig. 6*A*). These changes were roughly paralleled by the changes in the slow component of latent addition (Fig. 6*B*), and motor and sensory fibres showed a similar relationship between the two parameters (Fig. 6*D*). (The line in Fig. 6*D* is not based on the experimental data, but is the regression line for slow component *vs.* strength–duration time constant calculated for the model myelinated axon (Fig. 6*C*) described below (model 4).)

Models of latent addition

Model 1. Panizza *et al.* (1994) interpreted their latent addition results in terms of a simple passive membrane model, equivalent to our model 1. Membrane potential trajectories and latent addition for this type of model are illustrated in Fig. 7*A*. Latent addition is not always exponential for even this simple model, except in the 1st quadrant where a hyperpolarizing fixed pulse precedes the test pulse. For the depolarizing conditioning pulses in the 2nd quadrant, the waveforms are more complicated, since 'excitation' can occur at the end of the conditioning pulse rather than at the end of the test pulse. When a hyperpolarizing 'conditioning' pulse comes after the test pulse (4th quadrant) excitation can also occur at the start of the conditioning pulse. A full analysis of the latent addition waveforms for this model shows that they are made up of segments which follow one of six different equations, depending on the relative timing and amplitude of the test and conditioning pulses (see Appendix).

Model 2. For our second model (Fig. 7*B*), we added sodium channels with the kinetics described by Schwarz & Eikhof (1987) for rat nodes of Ranvier at 37 °C, which until recently appeared to be the best available model for mammalian myelinated axons *in vivo* (e.g. Bostock *et al.* 1991, 1994). Although this model generates realistic action potentials, and can exhibit a local response, latent addition to depolarizing pulses is improved surprisingly little compared with model 1.

Model 3. For our third model (Fig. 7*C*), we used sodium channel data derived from recordings from human nodes of Ranvier *in vitro* (Schwarz *et al.* 1995). (For this model, as for the previous two, the passive time constant was adjusted to match the fast time constant of latent addition *in vivo*.) This model provided a much better description of the responses

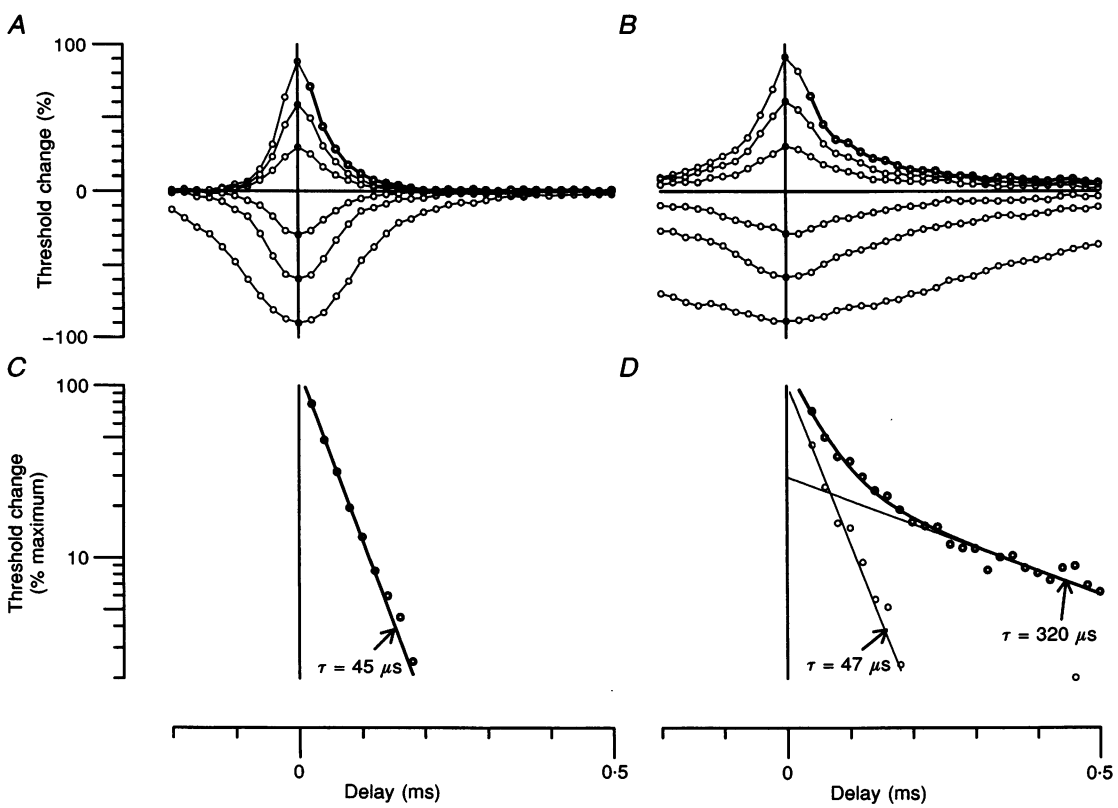

Figure 5. Effects of polarization on motor latent addition

Latent addition and exponential components for motor fibres in normal subject (different subject from Figs 1–3). *A* and *C*, latent addition recorded at end of 20 ms hyperpolarizing current (equivalent to half-threshold current for 1 ms pulses). *B* and *D*, latent addition recorded at end of similar 20 ms depolarizing current. Single (*C*) and double (*D*) exponential fits plotted as in Fig. 3.

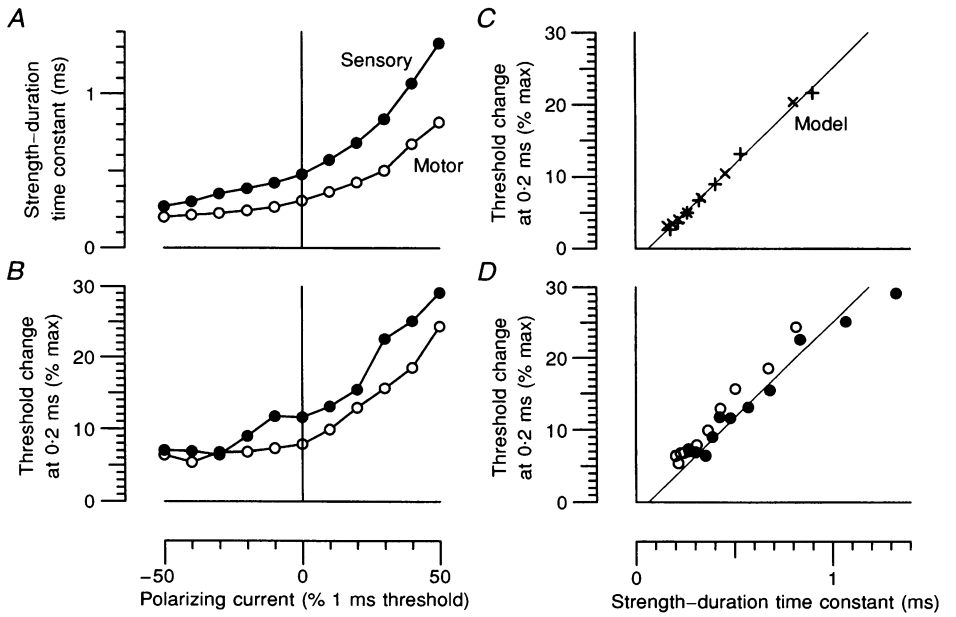

Figure 6. Effects of polarization on latent addition and strength–duration behaviour

A, strength–duration time constants for motor and sensory fibres, estimated from thresholds to 60 and 600 μs pulses, plotted as functions of 20 ms polarizing current (same subject as Fig. 5). *B*, slow components of latent addition, measured as the percentage change in threshold, 0·2 ms after a −90% hyperpolarizing pulse, plotted similarly. *C*, relationship between slow component of latent addition and strength–duration time constant for model axon, varying percentage threshold channels (+) or polarizing current (×) (see text). *D*, data replotted from *A* and *B* to show relationship between slow component of latent addition and strength–duration time constant for motor (○) and sensory (●) fibres. (Lines in *C* and *D* are the regression line for the model data in *C*: $y = -1{\cdot}7 + 26{\cdot}7x$).

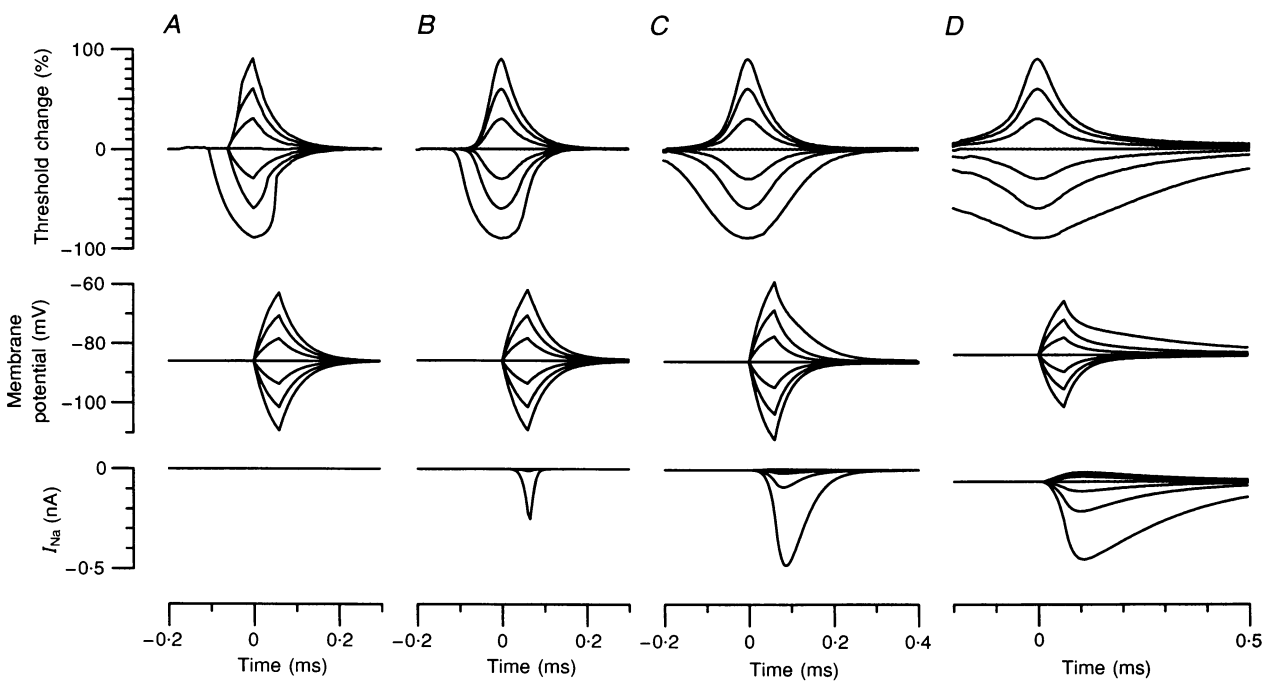

Figure 7. Mathematical models of latent addition

A, model 1 (passive membrane). *B*, model 2 (rat node). *C*, model 3 (human node). *D*, model 4 (human node with 2·5% threshold channels). Top: threshold change due to conditioning pulses, set to ±90, ±60 and ±30% of threshold, plotted as for *in vivo* data. Middle: membrane potential changes due to conditioning pulses. Bottom: sodium currents activated by conditioning pulses, including (in *D*) currents from threshold channels.

to depolarizing pulses, so that the latent addition waveforms in Fig. 7*C* superimpose almost perfectly on those in Fig. 5*A* recorded from hyperpolarized motor fibres. The single factor which accounted for most of the improvement in model 3 over model 2 was the voltage dependence of sodium channel activation (see Discussion).

Model 4. Replacement of 2·5% of normal sodium channels with 'threshold channels', with properties similar to neuronal persistent sodium channels (see Methods and Discussion) produced the voltage, current and latent addition waveforms in Fig. 7*D*. In this model the fibres were depolarized by about 1·5 mV relative to model 3, due to a small resting inward sodium current, which was deactivated by hyperpolarizing pulses to produce a slow component in the latent addition. These latent addition responses closely resembled those from sensory nerves *in vivo*, in both the prolongation of the local responses to depolarizing pulses, and in the slow, voltage-dependent component of the responses to hyperpolarizing pulses.

Figure 8*B* shows how recovery times of simulated latent addition differed between models, and how it depended on the proportion of sodium channels replaced by threshold channels for model 4. The corresponding threshold changes at 0·2 ms (corresponding roughly to the slow components for the hyperpolarizing conditioning pulses) are plotted in Fig. 8*D*. The mean motor and sensory *in vivo* responses (Fig. 8*A* and *C*) corresponded quite closely to model 4 with 1·0 and 2·5% threshold channels, respectively, and these values were taken as representative for the remaining modelling.

Fast and slow components of modelled latent addition

For the threshold channels to account satisfactorily for the difference between latent addition in motor and sensory fibres, the hyperpolarizing responses should be separable into fast and slow exponential components, corresponding to contributions of the passive membrane time constant and the threshold channels, respectively. Figure 9 shows the results of fitting exponentials to the representative motor and sensory models, with 1 and 2·5% threshold channels, respectively. Up to 0·5 ms, both −90% hyperpolarizing responses are well fitted by the sum of two exponentials, with indistinguishable fast time constants (47 and 48 μs). There is a suggestion in Fig. 9*D* that the model sensory response would deviate from the sum of two exponentials at greater delays, and this was borne out by extending the simulations. This is not surprising, since there is no

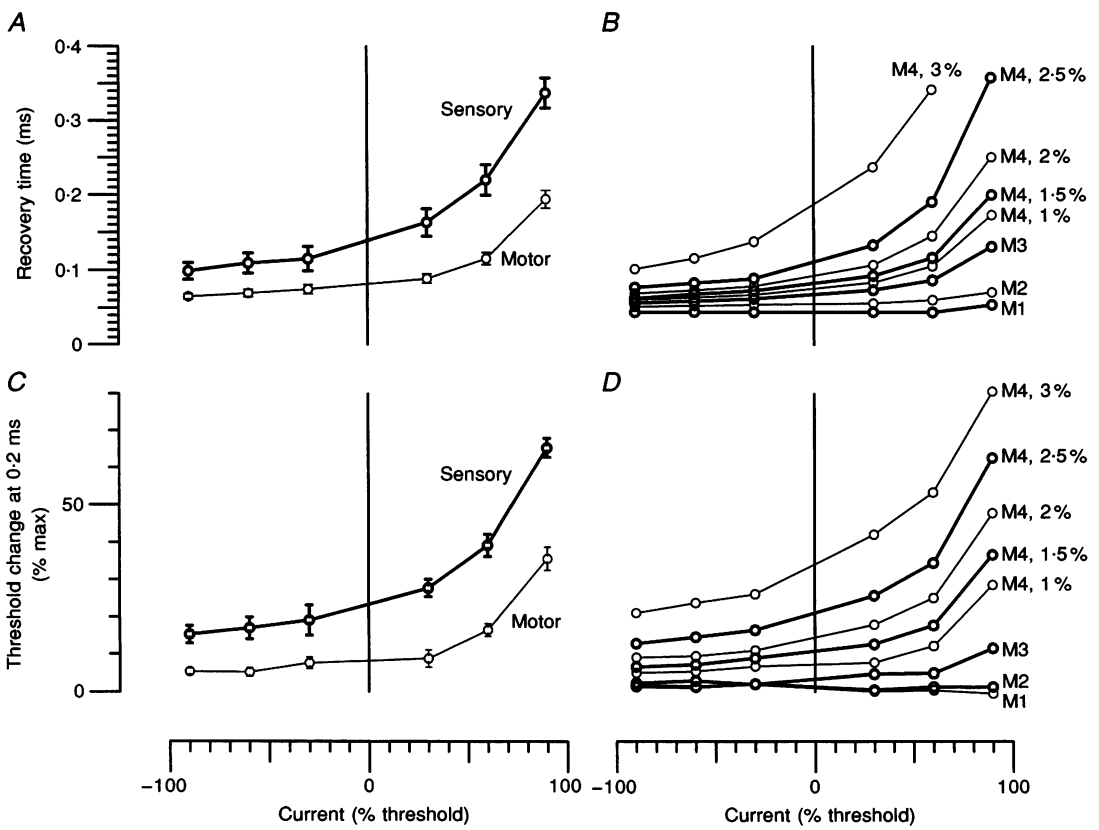

Figure 8. Comparison of latent addition *in vivo* with models: recovery times and slow components

A and *B*, recovery times measured as delay for recovery of threshold to 1/e of maximal value, as in Fig. 2*C* and *D*. *C* and *D*, threshold changes at 0·2 ms (when fast component negligible). *A* and *C*, average motor and sensory data for 9 normal subjects (means ± S.E.M.). *B* and *D*, data for models 1–3 (M1–M3) and for model 4 (M4) with 1–3% of sodium channels replaced by threshold channels.

theoretical expectation for the slow component to be a single exponential. We simply observe here that, up to a delay of 0·5 ms, latent addition to hyperpolarizing pulses in the model, like that in the human axons, is well fitted by two exponentials. The fast time constant for this model was somewhat longer than the theoretical resting input time constant ($R_{ll}C_{in}$, see Methods), which was 38 μs.

A further test of the threshold channels as the basis for the slow component of latent addition is that depolarizing and hyperpolarizing currents should alter the amplitude of the slow component but have little effect on the fast time constant, as in Fig. 5. We therefore tested the model motor fibre in a comparable way, by adding depolarizing and hyperpolarizing currents, equivalent to half the threshold for a 1 ms stimulus. The results are illustrated in Fig. 10*A*, and *B*, and the exponential components for the −90% responses are illustrated in Fig. 10*C* and *D*. As in Fig. 5, hyperpolarization eliminates the slow component (Fig. 10*C*) while depolarization enhances it (Fig. 10*D*), making the responses very similar to those of the sensory model in Fig. 9*B* and *D*.

The relationship between the slow component of latent addition and the strength–duration time constant was also tested for model 4, and found to be virtually identical, whether the amplitude of the slow component was changed by altering membrane potential or by altering the percentage of threshold channels (Fig. 6*C*). The + symbols were calculated for the model with 0–3% (in 0·5% steps) of sodium channels replaced by threshold channels, while the × symbols were calculated for the model with 1% of threshold channels, subject to steady-state polarizing currents from 0 to ±0·15 nA in 0·05 nA steps (corresponding to membrane potentials from −76·3 to −94·7 mV). All the calculated points lie close to the regression line ($y = -1{\cdot}7 + 26{\cdot}7x$), and the experimental points for motor and sensory fibres also lay close to this line (Fig. 6*D*). These results indicate the applicability of the model to strength–duration as well as latent addition data, but they also emphasize a limitation of the latent addition analysis in this study, i.e. that it is not possible to distinguish between depolarized motor fibres and sensory fibres. (Similarly, the difference in latent addition between motor and sensory fibres could be modelled by a difference in membrane potential, or by a difference in the voltage dependence of the threshold channels, as well as by a difference in their density.)

Effect of pulse duration on latent addition in the models and *in vivo*

A further test of the applicability of our models of latent addition is to change the 3rd parameter in our experimental protocol, namely pulse duration. In the subject illustrated in

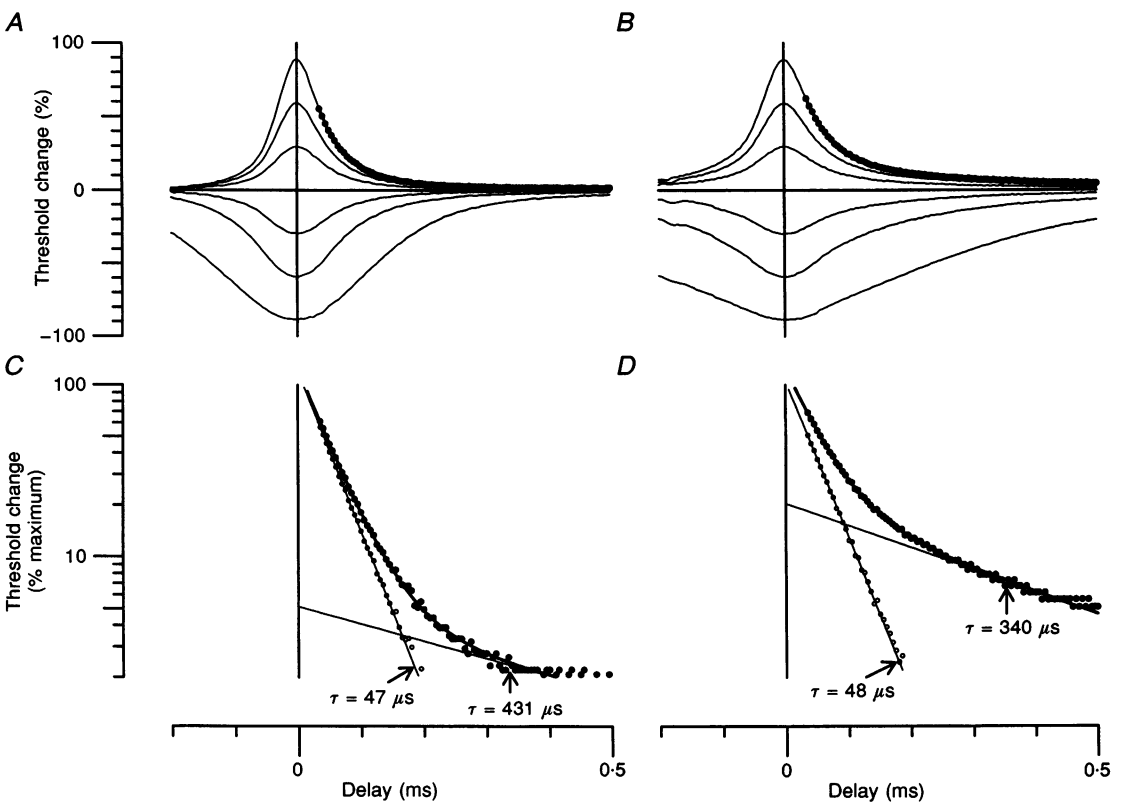

Figure 9. Exponential components of latent addition in model axons

A and *C*, latent addition for model motor fibre (model 4, 1% threshold channels), with separation of fast and slow components as in Fig. 3*B* and *D*. *B* and *D*, latent addition for model sensory fibre (model 4, 2·5% threshold channels) plotted similarly.

Fig. 2, whose latent addition results most closely matched the mean responses, we repeated the recordings using 200 μs rather than 60 μs conditioning and test pulses. The results are illustrated by the filled circles in Fig. 11*B* and *D* and show a distinct broadening of the cusps about zero delay, and marked delays in recovery. Both the 60 and 200 μs responses are well fitted by simulation with our standard motor and sensory models, illustrated by the continuous lines.

DISCUSSION

In this study we have used surface stimulation and recording to investigate the excitability properties of human motor and cutaneous sensory axons, to record an index of the local responses to subthreshold activation, and to infer the existence and some of the properties of a non-classical membrane conductance, apparently responsible for the motor–sensory differences. The human nerve *in vivo* may seem an unpromising preparation for investigating the biophysics of axonal membrane. However, despite its obvious disadvantages (e.g. multiunit preparation, currents applied through complex tissue impedance, no direct voltage measurement), this preparation has two important advantages: excellent long-term stability of membrane potential and excitability (with no danger of electrode damage), and a conspicuous difference between the apparent time constants of motor and sensory fibres. Panizza *et al.* (1994) estimated average strength–duration time constants in human sensory and motor fibres of 318 and 137 μs, respectively, whereas Erlanger & Blair (1938) reported much closer corresponding values in a typical frog nerve of 190 and 160 μs. The effects of tissue impedance are not easily estimated, but the correspondence between the human data and models in this study could not be improved by making allowances for high-pass or low-pass filtering of the applied currents by the tissues, so we have assumed that any such filtering was negligible.

The disadvantages of a multi-unit preparation for determining excitability changes to be related to those in a single axon model are more apparent than real. The virtue of the 'threshold tracking' (constant response) method of determining electrical excitability is that 'threshold' changes measured for compound action potentials can be related directly to those in constituent fibres. By setting the target response to 35% of the maximal response, we were effectively tracking the threshold of an axon (the 'target axon') recruited at that level of response. However, because the stimulus–response relationship is steepest at this point, due to the recruitment of many axons with a small increase

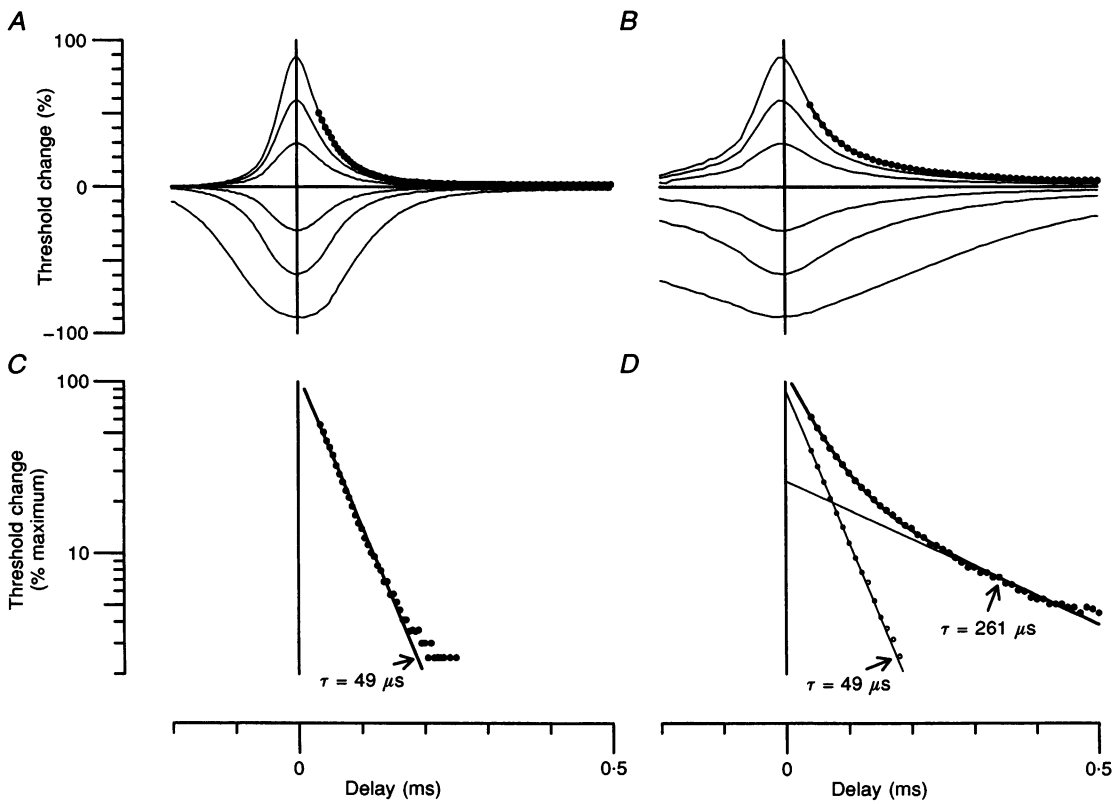

Figure 10. Effects of polarization on latent addition in model axon

A and *C*, latent addition in hyperpolarized model motor fibre, to compare with Fig. 5*A* and *C*. *B* and *D*, latent addition in depolarized model motor fibre (cf. Fig. 5*B* and *D*). (Corresponding records for the unpolarized model motor fibre were illustrated in Fig. 9*A* and *C*.)

in stimulus, this threshold actually depends on many fibres and can be determined more precisely than that of a single fibre (for which the threshold typically fluctuates over a 10% range from moment to moment (Bergmans, 1970)). In the latent addition experiments, responses are measured to a conditioning + test stimulus pair, and it does not matter whether part of that response comes from axons excited by the conditioning stimulus alone (as with the stronger depolarizing conditioning pulses) or not, provided that all the fibres with thresholds below that of the target axon contribute one action potential, and one action potential only, to the response at threshold. By limiting our conditioning–test intervals to a maximum of 0·5 ms, we ensured that no fibre was excited by both the conditioning and the test stimuli, and no significant error was incurred due to temporal dispersion of the responses over the 0·5 ms interval.

Importance of local response for latent addition and strength–duration behaviour

According to Tasaki (1950), who investigated latent addition in isolated frog fibres, local responses only make a significant contribution to the excitability changes for stimuli above 50% of threshold, while below that level he found that latent addition to depolarizing stimuli closely mirrored that to hyperpolarizing stimuli. We found that this was approximately the case for motor fibres, but not for the sensory fibres, which showed a significant asymmetry, even between the ±30% responses (e.g. Fig. 2*D*).

Even in the motor fibres, stimuli above 50% of threshold caused a much more prolonged increase in excitability, and the likely nature of the underlying local response, due to sodium channel activation, can be appreciated by comparing the model responses in Fig. 7. A critical variable in the model was the voltage dependence of sodium channel activation. Model 1, like that of Panizza *et al.* (1994), is equivalent to the assumption that the sodium channel activation curve is infinitely steep, giving a sharp voltage threshold for spike initiation; this reproduces the exponential responses to hyperpolarizing stimuli, but provides only a very inadequate model of the depolarizing responses. Model 2, based on the equations of Schwarz & Eikhof (1987) for rat nodes, is slightly better, but model 3, based on human nodal sodium currents (Schwarz *et al.* 1995), provides a much more accurate description of the motor latent addition data. Schwarz *et al.* (1995) reduced sodium currents with 3 nM tetrodotoxin (TTX) to minimize the series resistance artifact and, as discussed by them and Neumcke, Schwarz & Stämpfli (1987), this has the effect of reducing the steepness

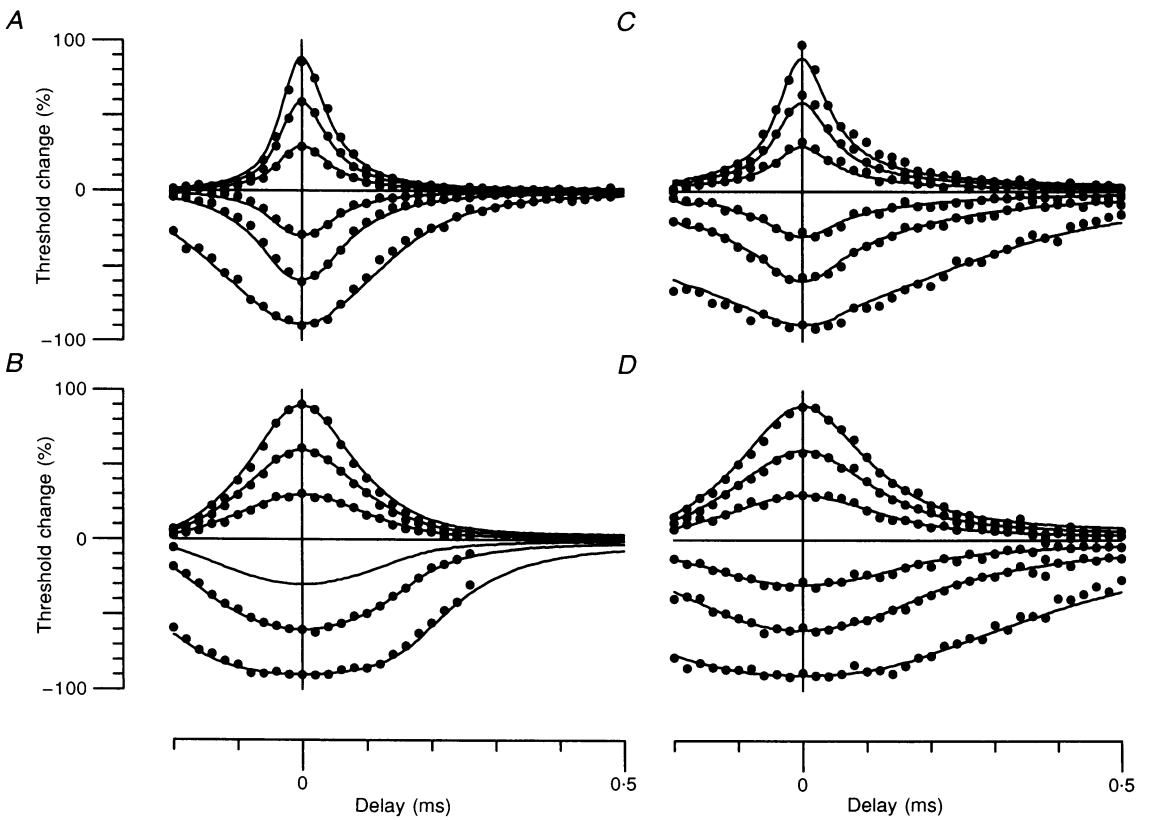

Figure 11. Effect of pulse duration on latent addition in human and model axons

Filled circles represent data recorded from normal subject (same as Fig. 2), while lines are derived from standard motor and sensory models (i.e. model 4 with 1 and 2·5% threshold channels, as in Fig. 9). *A* and *C*, 60 μs test and conditioning stimuli. *B* and *D*, 200 μs stimuli. *A* and *B*, motor. *C* and *D*, sensory.

of the sodium activation (m_∞ *vs.* membrane potential) curve. Schwarz & Eikhof (1987) did not take steps to minimize the series resistance artifact, so the improvement in model 3 over model 2 most probably reflects a difference in quality of the voltage clamp recordings, rather than a genuine difference between human and rat sodium channels. The functional importance of the local response is indicated by the strength–duration behaviour: for models 2, 3, 4 (motor) and 4 (sensory), the strength–duration time constants for a fibre with a passive membrane time constant of 45 μs were estimated as 49, 176, 262 and 535 μs, respectively.

Fast and slow time constants of latent addition

A surprising new result in this study was the finding that after hyperpolarizing pulses the thresholds did not in general recover exponentially, but as the sum of two exponentials. A fast exponential component of recovery, with a time constant in the range 32–60 μs, was present for all responses, motor or sensory. These fast time constants (mean 43·3 μs) provide much more plausible estimates for the passive input time constants of the fibres than those estimated with depolarizing pulses by Panizza *et al.* (1994), which ranged from 53 to 642 μs, with means of 148 μs (motor) and 349 μs (sensory). However, our modelling suggested that even the fast components of the hyperpolarizing responses were slightly dependent on sodium channels.

The origin of the slow exponential component of recovery from hyperpolarizing pulses, which was more pronounced in sensory fibres and sometimes absent in motor fibres, was more mysterious. A second passive membrane time constant seemed unlikely, firstly because no structural difference between motor and sensory myelinated axons has been described which could account for it, and secondly because the proportion of slow component depends on the amplitude of the hyperpolarizing pulses (Table 1 and Fig. 8*C*), implicating a voltage-dependent process. The voltage dependence was shown more directly by the effects of polarizing currents, which could eliminate the differences in the slow component between motor and sensory fibres (Figs 5 and 6). To model the second time constant, we therefore considered the likelihood that it was caused by voltage-dependent ion channels, which could delay recovery to hyperpolarizing pulses in the same way that the local response of normal sodium channels delays recovery to depolarizing pulses. From our latent addition data we could deduce a partial profile of these hypothetical channels: (a) they must be active at the resting potential (at least in sensory fibres) so that they can affect the responses to hyperpolarizing as well as depolarizing currents; (b) they must be regenerative (i.e. a hyperpolarization-activated outward current or a depolarization-activated inward current), acting to enhance and prolong the effects of applied currents, so they are presumably sodium or calcium channels; (c) they activate and deactivate very quickly, to be affected by our 60 μs pulses; and (d) they do not inactivate much, at least at potentials subthreshold for spike initiation.

A second type of sodium channel?

Channels or currents with at least some of these properties have been described in a number of axonal and neuronal preparations. Dubois & Bergman (1975) described a 'late sodium current' at amphibian nodes of Ranvier, a TTX-sensitive inward current that persisted for at least 300 ms after a depolarizing pulse, and was more marked in sensory than motor fibres. They proposed that there were two populations of sodium channels in the nodal membrane, and that about 2% of sodium channels were activated at potentials at least 10 mV more negative than normal and failed to inactivate. Curiously, this current has not figured in more recent voltage clamp studies on myelinated axons (Vogel & Schwarz, 1995), although evidence from extracellularly recorded membrane potentials for a TTX-sensitive, non-inactivating inward current has been found in rat optic nerve (Stys, Sontheimer, Ransom & Waxman, 1993) and in rat dorsal roots (Grafe, Bostock & Schneider, 1994).

A non-inactivating, low-threshold sodium conductance was proposed by Llinas & Sugimori (1980) to account for the electrical properties of cerebellar Purkinje cells. Low-threshold, persistent sodium currents have since been described in many other neuronal cell types, and in skeletal and heart muscle cells (Stafstrom, Schwindt & Crill, 1982; Stafstrom, Schwindt, Chubb & Crill, 1985; Gage, Lamb & Wakefield, 1989; French, Sah, Buckett & Gage, 1990; Saint, Ju & Gage, 1992; Taylor, 1993). A low-threshold, persistent current in squid axon was attributed to 'threshold channels' by Gilly & Armstrong (1984), because these channels 'must dominate the behaviour of the axon membrane in the threshold region for spike initiation'. Their term, which emphasizes the functional importance of such channels, seems appropriate for the hypothetical channels responsible for the slow component of latent addition, since our data provide no information on the type of ion involved.

The persistent sodium (Na_P) current in Purkinje cells has recently been modelled by de Schutter & Bower (1994), using equations based on voltage clamp data from hippocampal neurones (French *et al.* 1990) as well as Purkinje cells (Kay, Sugimori & Llinas, 1990). In relation to the normal sodium channels in that preparation, activation of the persistent sodium channels occurred at potentials about 20 mV more negative, and at about half the rate, and they did not inactivate. We used these simple assumptions to model the threshold channels in human axons in our model 4. We found that if 2·5% of the sodium channels in our model were given these properties, latent addition to both depolarizing and hyperpolarizing pulses closely resembled that of a typical sensory nerve, while a smaller proportion of threshold channels was appropriate for motor nerves (Figs 8 and 9). Moreover, the modelled hyperpolarizing responses resembled the responses from human axons in that they behave as the sum of fast and slow components (Fig. 9) and in the sensitivity of the slow component to polarization (Fig. 10). Finally, the predictive value of this model extended to latent addition recorded

with much longer duration current pulses (Fig. 11), and to the relationship between the slow component of latent addition to hyperpolarizing pulses and the strength–duration time constant (Fig. 6). We conclude that both the kinetics and the voltage dependence of the threshold channels in the model must be in good agreement with the active membrane properties of the axons close to the resting potential. However, it is notable that latent addition in depolarized motor fibres was indistinguishable from that in normal sensory fibres, both in our model (Figs 9*B* and 10*B*) and *in vivo* (Figs 3*B* and 5*B*), so that although we have modelled the motor–sensory difference by a difference in density of threshold channels, our results are also compatible with the sensory fibres being relatively depolarized, or having threshold channels that are activated at relatively more negative potentials. Similarly, our data cannot be used to distinguish whether the hypothesized threshold channels are discrete molecular entities, as seems likely in heart muscle (Saint *et al.* 1992), or whether they represent a different gating mode of transient sodium channels, as has been suggested for some neuronal persistent sodium currents (Alzheimer, Schwindt & Crill, 1993).

Some of these questions about the nature of the axonal 'threshold channels' may soon be answered by an indirect voltage clamp approach. Following our preliminary results, Baker & Bostock (1996) have looked for evidence of these channels in large (50–75 μm diameter) rat dorsal root gangion cells, the presumed cell bodies of large cutaneous and motor afferent fibres in peripheral nerve. Whole-cell patch clamp recordings have demonstrated the presence in almost half of these cells of a TTX-sensitive, low-threshold, persistent sodium current, with properties very similar to those assumed in our model 4.

Relevance of latent addition results to other motor–sensory differences

An important functional difference between motor and sensory fibres, which was already well known 125 years ago, is that sensory fibres have a greater tendency to fire repetitively during a sustained depolarization (Bostock, 1995). This difference in 'repetitiousness' was analysed by Erlanger & Blair (1938), who related it to two other differences they found in frog nerve: a difference in rheobase, with sensory fibres being more excitable than motor fibres of similar diameter, and a difference in strength–duration time constant, with sensory fibres being preferentially excited by currents of longer duration. These three differences are also found in humans, with only sensory fibres normally discharging repetitively during ischaemia or application of DC currents, and with the differences in rheobase and strength–duration time constants previously mentioned (Mogyoros *et al.* 1996). Although some of the motor–sensory differences in frog nerve may be attributable to differences in potassium channels, this seems implausible in human peripheral nerve, where fast potassium channels are thought to be poorly represented at the nodes of Ranvier (Schwarz *et al.* 1995), and where accommodation due to activation of slow potassium channels is very similar in motor and sensory fibres (Bostock *et al.* 1994).

It seems likely that the threshold channels inferred in this study make a major contribution to all three types of motor–sensory difference described by Erlanger & Blair (1938), although we have only tested directly for a relationship between latent addition and strength–duration time constant (Fig. 6). In our model, the addition of threshold channels directly depolarizes the axon because of the resting inward current, and both this resting depolarization and the further activation of these channels by depolarizing pulses contribute to a lowering of rheobase. Thus the estimated rheobase of model 3 (human Na^+ channels only) was 0·47 nA per internode, while conversion of 1 and 2·5% of these Na^+ channels to threshold channels lowered the rheobase to 0·31 and 0·12 nA, respectively. We have not yet investigated the effects of the threshold channels on repetitive firing in our model, but they can be expected to increase repetitiousness. In cerebellar Purkinje cells, de Schutter & Bower (1994) found that their persistent sodium channels, the model for our threshold channels, facilitated repetitive firing to a maintained current. Our observation that one subject who was known to produce repetitive motor discharges during ischaemia also had motor axons with a sensory pattern of latent addition (Fig. 4) is suggestive, but we have not attempted to test for a relationship between these phenomena in other subjects.

In conclusion, our latent addition results and modelling lead us to propose that human cutaneous afferents contain a small but significant proportion of 'threshold channels', similar to neuronal persistent sodium channels, which are partially active at the resting potential, and enhance local responses and increase the strength–duration time constant. Motor fibres normally have less evidence of threshold channels active at the resting potential, although they can be activated by depolarization. This probably reflects a smaller proportion of these channels (or that the sodium channels spend a smaller proportion of their time in this gating mode), but could also result from a difference in activation voltage relative to the resting potential.

APPENDIX

Latent addition for passive membrane (model 1)

Panizza *et al.* (1994) derived an expression for latent addition, limited to the situation where the test stimulus is delivered at or after the end of the conditioning stimulus. Here we will derive expressions to cover the general case of excitation by two pulses of the same duration, allowing the pulses to overlap, allowing for the conditioning stimulus to be delivered after as well as before the test stimulus, and allowing for the conditioning stimulus to be hyperpolarizing as well as depolarizing, to cover the range of conditioning stimuli used experimentally.

Let w = duration of test and conditioning stimuli

t = time relative to onset of conditioning stimulus

d = time from onset of conditioning stimulus to onset of test stimulus

τ = membrane time constant

C = conditioning stimulus as fraction of control threshold stimulus

S = test stimulus as fraction of control threshold stimulus

T = value of S at threshold

$V(t)$ = depolarization as fraction of threshold depolarization

$V_C(t)$ = portion of $V(t)$ due to conditioning stimulus

$V_S(t)$ = portion of $V(t)$ due to test stimulus.

The conditioning and test stimuli are assumed to produce potential changes which increase exponentially, with time constant τ, to a maximum (C,T) after time w, and then decay exponentially, also with time constant τ, i.e.:

$$V_C(t) = 0 \quad \text{for:} \quad t \leqslant 0 \tag{1a}$$

$$V_C(t) = C(1-e^{-t/\tau})/(1-e^{-w/\tau}) \quad 0 \leqslant t \leqslant w \tag{1b}$$

$$V_C(t) = C \quad t = w \tag{1c}$$

$$V_C(t) = Ce^{-(t-w)/\tau} \quad t \geqslant w \tag{1d}$$

$$V_S(t) = S(1-e^{-(t-d)/\tau})/(1-e^{-w/\tau}) \quad 0 \leqslant t-d \leqslant w \tag{2a}$$

$$V_S(t) = S \quad t-d = w \tag{2b}$$

$$V_S(t) = Se^{-(t-d-w)/\tau} \quad t-d \geqslant w \tag{2c}$$

and: $V(t) = V_C(t) + V_S(t)$. (3)

As illustrated in Fig. 12, excitation can occur at the end of the test pulse (A), at the end of the conditioning pulse (B and C), or (if the conditioning pulse is hyperpolarizing) at the start of the conditioning pulse (D). Different equations result for the following different situations.

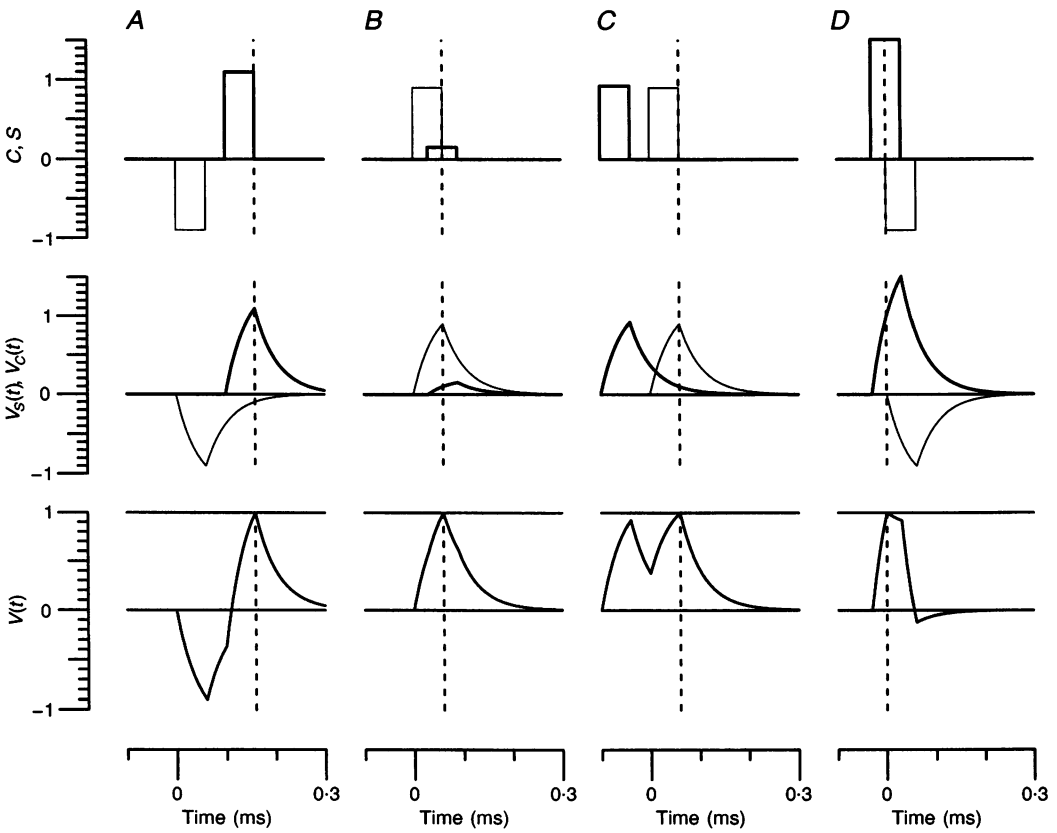

Figure 12. Latent addition in a passive membrane

Latent addition in model 1, showing different times at which excitation can occur, depending on conditioning–test pulse delay (d) and amplitude of conditioning pulse, as a fraction of threshold (C). *A*: $C = -0{\cdot}9$, $d = 0{\cdot}1$ ms, excitation at end of test pulse. *B*: $C = 0{\cdot}9$, $d = 0{\cdot}03$ ms, excitation at end of conditioning pulse. *C*: $C = 0{\cdot}9$, $d = -0{\cdot}1$ ms, excitation at end of conditioning pulse. *D*: $C = -0{\cdot}9$, $d = -0{\cdot}03$ ms, excitation at start of conditioning pulse. Top: conditioning (C, thin lines) and test (S, thick lines) stimulus waveforms. Middle: corresponding membrane potential changes ($V_C(t)$, thin lines; $V_S(t)$, thick lines). Bottom: membrane potential change due to sum of conditioning and test stimuli. Currents and voltages expressed as fractions of threshold values, plotted against time (t) from start of conditioning stimulus. Vertical dashed lines indicate time of excitation.

Excitation at end of test pulse

At end of test pulse:

$$t = w + d. \quad (4)$$

From eqns (2b and 3): $V(t) = V_C(t) + S.$ (5)

When $d > 0$ (i.e. end of test pulse occurs during falling phase of conditioning pulse, e.g. Fig. 12*A*) then:

From eqn (4): $t > w.$

From eqn (1d): $V_C(t) = Ce^{-(t-w)/\tau}.$

From eqn (5): $V(t) = Ce^{-(t-w)/\tau} + S.$

At threshold, $S = T$ and $V(t) = 1$, so:

$$T = 1 - Ce^{-d/\tau}. \quad (6)$$

This equation corresponds to eqn (A10) of Panizza *et al.* (1994).

When $-w < d < 0$ (i.e. end of test pulse occurs during rising phase of conditioning pulse) then:

From eqn (4): $0 < t < w.$

From eqn (1b): $V_C(t) = C(1-e^{-t/\tau})/(1-e^{-w/\tau}).$

From eqn (5): $V(t) = C(1-e^{-t/\tau})/(1-e^{-w/\tau}) + S.$

At threshold, $S = T$ and $V(t) = 1$, so:

$$T = 1 - C(1-e^{-(w+d)/\tau})/(1-e^{-w/\tau}). \quad (7)$$

When $d < -w$ (i.e. end of test pulse occurs before the start of the conditioning pulse) then the conditioning pulse makes no contribution to stimulation and at threshold:

$$T = 1. \quad (8)$$

Excitation at the end of the conditioning pulse

At the end of the conditioning pulse:

$$t = w. \quad (9)$$

From eqns (1c) and (3): $V(t) = V_S(t) + C.$ (10)

When $0 < d < w$ (i.e. end of conditioning pulse occurs during rising phase of test pulse, e.g. Fig. 12*B*) then:

From eqn (9): $0 < t - d < w.$

From eqn (2a): $V_S(t) = S(1-e^{-(t-d)/\tau})/(1-e^{-w/\tau}).$

From eqns (9) and (10): $V(t) = S(1-e^{-(w-d)/\tau})/(1-e^{-w/\tau}) + C.$

At threshold, $S = T$ and $V(t) = 1$, so:

$$T = (1-C)(1-e^{-w/\tau})/(1-e^{-(w-d)/\tau}). \quad (11)$$

When $d < 0$ (i.e. end of conditioning pulse occurs during falling phase of test pulse, e.g. Fig. 12*C*) then:

From eqn (9): $t - d > w.$

From eqn (2c): $V_S(t) = Se^{-(t-d-w)/\tau}.$

From eqns (9) and (10): $V(t) = Se^{d/\tau} + C.$

At threshold, $S = T$ and $V(t) = 1$, so:

$$T = (1-C)e^{-d/\tau}. \quad (12)$$

Excitation at the start of the conditioning pulse

At the start of the conditioning pulse:

$$t = 0. \quad (13)$$

From eqns (1a) and (3): $V(t) = V_S(t).$ (14)

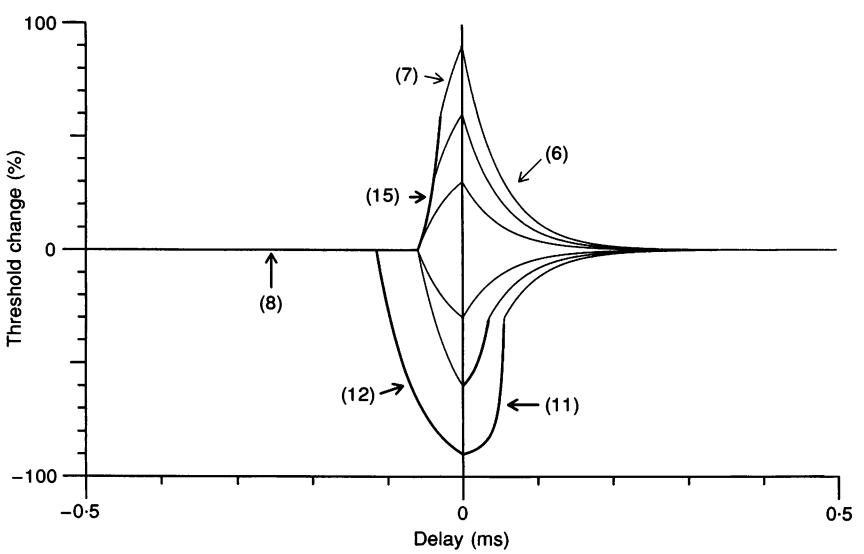

Figure 13. Theoretical latent addition in a passive membrane

Latent addition in model 1, calculated from the six derived equations. Numbers in parentheses refer to equations in text. Equations (6), (7) and (8) apply when excitation occurs at the end of the test pulse, eqns (11) and (12) when excitation occurs at the end of the conditioning pulse, and eqn (15) when a hyperpolarizing conditioning pulse occurs during the rising phase of the test pulse and excitation occurs at the start of the conditioning pulse. These theoretical responses correspond closely to those simulated in Fig. 7*A*.

When $-w < d < 0$ (i.e. start of conditioning pulse occurs during rising phase of test pulse, e.g. Fig. 12*D*) then:

From eqn (13): $0 < t - d < w$.

From eqn (2a): $V_S(t) = S(1-e^{-(t-d)/\tau})/(1-e^{-w/\tau})$.

From eqns (13) and (14): $V(t) = S(1-e^{d/\tau})/(1-e^{-w/\tau})$.

At threshold, $S = T$ and $V(t) = 1$, so:

$$T = (1-e^{-w/\tau})/(1-e^{d/\tau}). \quad (15)$$

The threshold current for any particular combination of d, w, τ and C is given by whichever of the applicable equations has the minimum value.

Thus for:

$d > w$	T is given by eqn (6).
$0 < d < w$	T is given by minimum of eqns (6) and (11).
$-w < d < 0$	T is given by minimum of eqns (7), (12) and (15).
$d < -w$	T is given by minimum of eqns (8) and (12).

A program was written to evaluate and select between these expressions, for the case of $w = 60$ μs, $\tau = 45$ μs, $C = -0{\cdot}9$, $-0{\cdot}6$, $-0{\cdot}3$, $0{\cdot}3$, $0{\cdot}6$ and $0{\cdot}9$, and for values of d from $-0{\cdot}2$ to $0{\cdot}5$ ms, corresponding to our standard latent addition protocol, and the results are plotted in Fig. 13. The curves correspond accurately to those generated for model 1 by threshold tracking and illustrated in Fig. 7*A*.

ALZHEIMER, C., SCHWINDT, P. & CRILL, W. E. (1993). Modal gating of Na^+ channels as a mechanism of persistent Na^+ current in pyramidal neurons from rat and cat sensorimotor cortex. *Journal of Neuroscience* **13**, 660–673.

BAKER, M. D. & BOSTOCK, H. (1996). Sustained inward currents in large neurones cultured from adult rat dorsal root ganglia. *Journal of Physiology* **491.P**, 141–142*P*.

BARRETT, E. F. & BARRETT, J. N. (1982). Intracellular recordings from vertebrate myelinated axons: mechanism of the depolarizing after-potential. *Journal of Physiology* **323**, 117–144.

BERGMANS, J. (1970). *The Physiology of Single Human Nerve Fibres.* Vander, University of Louvain, Belgium.

BOSTOCK, H. (1983). The strength–duration relationship for excitation of myelinated nerve: computed dependence on membrane parameters. *Journal of Physiology* **341**, 59–74.

BOSTOCK, H. (1995). Mechanisms of accommodation and adaptation in myelinated axons. In *The Axon*, ed. WAXMAN, S. G., STYS, P. K. & KOCSIS, J. D., pp. 311–327. Oxford University Press, Oxford, UK.

BOSTOCK, H., BAKER, M. & REID, G. (1991). Changes in excitability of human motor axons underlying post-ischaemic fasciculations: evidence for two stable states. *Journal of Physiology* **441**, 537–557.

BOSTOCK, H. & BERGMANS, J. (1994). Post-tetanic excitability changes and ectopic discharges in a human motor axon. *Brain* **117**, 913–928.

BOSTOCK, H., BURKE, D. & HALES, J. P. (1994). Differences in behaviour of sensory and motor axons following release of ischaemia. *Brain* **117**, 225–234.

BOSTOCK, H. & ROTHWELL, J. C. (1995). The time constants of motor and sensory axons in human peripheral nerve. *Journal of Physiology* **487.P**, 47*P*.

BOSTOCK, H., SEARS, T. A. & SHERRATT, R. M. (1983). The spatial distribution of excitability and membrane current in normal and demyelinated mammalian nerve fibres. *Journal of Physiology* **341**, 41–58.

BOSTOCK, H., SHARIEF, M. K., REID, G. & MURRAY, N. M. F. (1995). Axonal ion channel dysfunction in amyotrophic lateral sclerosis. *Brain* **118**, 217–225.

BRISMAR, T. (1981). Electrical properties of isolated demyelinated rat nerve fibres. *Acta Physiologica Scandinavica* **113**, 161–166.

DE SCHUTTER, E. & BOWER, J. M. (1994). An active membrane model of the cerebellar Purkinje cell. I. Simulation of current clamps in slice. *Journal of Neurophysiology* **71**, 375–400.

DUBOIS, J. M. & BERGMAN, C. (1975). Late sodium current in the Node of Ranvier. *Pflügers Archiv* **357**, 145–148.

ERLANGER, J. & BLAIR, E. A. (1938). Comparative observations on motor and sensory fibers with special reference to repetitiousness. *American Journal of Physiology* **121**, 431–453.

FRENCH, C. R., SAH, P., BUCKETT, K. J. & GAGE, P. W. (1990). A voltage-dependent perisitent sodium current in mammalian hippocampal neurons. *Journal of General Physiology* **95**, 1139–1157.

GAGE, P. W., LAMB, G. D. & WAKEFIELD, B. T. (1989). Transient and persistent sodium currents in normal and denervated mammalian skeletal muscle. *Journal of Physiology* **418**, 427–439.

GILLY, W. F. & ARMSTRONG, C. M. (1984). Threshold channels – a novel type of sodium channel in squid giant axon. *Nature* **309**, 448–450.

GRAFE, P., BOSTOCK, H. & SCHNEIDER, U. (1994). The effects of hyperglycaemic hypoxia on rectification in rat dorsal root axons. *Journal of Physiology* **480**, 297–307.

KATZ, B. (1937). Experimental evidence for a non-conducted response of nerve to subthreshold stimulation. *Proceedings of the Royal Society* B **124**, 244–276.

KAY, A. R., SUGIMORI, M. & LLINAS, R. (1990). Voltage clamp analysis of a persistent TTX-sensitive Na current in cerebellar Purkinje cells. *Society for Neuroscience Abstracts* **16**, 182.

LLINAS, R. & SUGIMORI, M. (1980). Electrophysiological properties of *in vitro* Purkinje cell somata in mammalian cerebellar slices. *Journal of Physiology* **305**, 171–195.

MOGYOROS, I., KIERNAN, M. & BURKE, D. (1996). Strength–duration properties of human peripheral nerve. *Brain* **119**, 439–447.

NEUMCKE, B., SCHWARZ, J. R. & STÄMPFLI, R. (1987). A comparison of sodium currents in rat and frog myelinated nerve: normal and modified sodium inactivation. *Journal of Physiology* **382**, 175–191.

PANIZZA, M., NILSSON, J. & HALLETT, M. (1989). Optimal stimulus duration for H reflexes. *Muscle and Nerve* **12**, 576–579.

PANIZZA, M., NILSSON, J., ROTH, B. J., BASSER, P. J. & HALLETT, M. (1992). Relevance of stimulus duration for activation of motor and sensory fibers: implications for the study of H-reflexes and magnetic stimulation. *Electroencephalography and Clinical Neurophysiology* **85**, 22–29.

PANIZZA, M., NILSSON, J., ROTH, B. J., ROTHWELL, J. & HALLETT, M. (1994). The time constants of motor and sensory peripheral nerve fibers measured with the method of latent addition. *Electroencephalography and Clinical Neurophysiology* **93**, 147–154.

SAINT, D. A., JU, Y.-K. & GAGE, P. W. (1992). A persistent sodium current in rat ventricular myocytes. *Journal of Physiology* **453**, 219–231.

Schwarz, J. R. & Eikhof, G. (1987). Na currents and action potentials in rat myelinated nerve fibres at 20 and 37 °C. *Pflügers Archiv* **409**, 569–577.

Schwarz, J. R., Reid, G. & Bostock, H. (1995). Action potentials and membrane currents in the human node of Ranvier. *Pflügers Archiv* **430**, 283–292.

Stafstrom, C. E., Schwindt, P. C., Chubb, M. C. & Crill, W. E. (1985). Properties of persistent sodium conductance and calcium conductance of layer V neurons from cat sensorimotor cortex *in vitro*. *Journal of Neurophysiology* **53**, 153–170.

Stafstrom, C. E., Schwindt, P. C. & Crill, W. E. (1982). Negative slope conductance due to a persistent subthreshold sodium current in cat neocortical neurons *in vitro*. *Brain Research* **236**, 221–226.

Stys, P. K., Sontheimer, H., Ransom, B. R. & Waxman, S. G. (1993). Noninactivating, tetrodotoxin-sensitive Na^+ conductance in rat optic nerve axons. *Proceedings of the National Academy of Sciences of the USA* **90**, 6976–6980.

Tasaki, I. (1939). The strength–duration relation of the normal, polarized and narcotized nerve fiber. *American Journal of Physiology* **126**, 367–379.

Tasaki, I. (1950). Nature of the local excitatory state in the nerve fiber. *Japanese Journal of Physiology* **1**, 75–85.

Taylor, C. P. (1993). Na^+ currents that fail to inactivate. *Trends in Neurosciences* **16**, 455–460.

Veale, J. L., Mark, R. F. & Rees, S. (1973). Differential sensitivity of motor and sensory fibres in human ulnar nerve. *Journal of Neurology, Neurosurgery and Psychiatry* **36**, 75–86.

Vogel, W. & Schwarz, J. R. (1995). Voltage-clamp studies on axons: macroscopic and single-channel currents. In *The Axon*, ed. Waxman, S. G., Stys, P. K. & Kocsis, J. D., pp. 257–280. Oxford University Press, Oxford.

Acknowledgements

This study was supported by The Wellcome Trust. We thank Dr M. D. Baker and Dr D. I. Stephanova for helpful discussions.

Author's email address

H. Bostock: hbostock@ion.ucl.ac.uk

Received 8 February 1996; accepted 9 September 1996.